



MONITORED AND MODELED CORRELATIONS OF SEDIMENT AND NUTRIENTS WITH CHESAPEAKE BAY WATER CLARITY¹

Ping Wang, Lewis C. Linker, and Richard A. Batiuk²

ABSTRACT: This article analyzes the correlations of the observed and modeled light attenuation coefficient, K_d , with *in situ* total suspended solids (TSS) and chlorophyll-*a* concentrations in Chesapeake Bay (CB) tidal waters, and with sediment and nutrient loads from the Chesapeake watershed. Light attenuation is closely related to *in situ* TSS and chlorophyll-*a* concentrations, however, the strength of the correlation differs among the CB segments. There are distinct differences between saline and tidal fresh segments in the main Bay, but less distinction among saline and tidal fresh segments in the tidal tributaries. The correlation between K_d with sediment and nutrient loads is complicated by the lag times of TSS and the chlorophyll-*a* responses to reductions in nutrient and sediment loads from the watershed, and also due to the diverse load sources. Three sets of model sensitivity scenarios were performed with: (1) differential sediment and nutrient loads; (2) selective sediment source types; and (3) geographically isolated inputs. The model results yield similar findings as those based on observed data and provide information regarding the effect of sediment on specific water bodies. Based on the model results a method was developed to determine sediment and nutrient load reductions needed to achieve the water clarity standards of the CB segments.

(KEY TERMS: water clarity; sediment loads; nutrient loads; TMDL; monitoring and modeling.)

Wang, Ping, Lewis C. Linker, and Richard A. Batiuk, 2013. Monitored and Modeled Correlations of Sediment and Nutrients with Chesapeake Bay Water Clarity. *Journal of the American Water Resources Association* (JAWRA) 1-16. DOI: 10.1111/jawr.12104

INTRODUCTION

The Chesapeake Bay (CB) Total Maximum Daily Load (TMDL) is based on achievement of Delaware, District of Columbia, Maryland, and Virginia's CB water quality standards for dissolved oxygen (DO), chlorophyll-*a*, and submerged aquatic vegetation (SAV)/water clarity (USEPA, 2010). The three water quality standards will ultimately be achieved through control of watershed sources of nutrient and sediment loads as well as controls on nitrogen (N) air emissions

leading to atmospheric deposition to the watershed and tidal waters of the Chesapeake. The CB estuary is divided into segments (CB segments) based on salinity, geographic location, and state boundaries (Figure 1) (USEPA, 2004). Each CB segment has specific TMDL designated uses assigned to it along with protective water quality criteria (Tango and Batiuk, this issue). There are 92 TMDL segments for the DO and clarity water quality standards (Linker *et al.*, this issue). For a more detailed SAV/water clarity assessment, some shallow areas were subdivided yielding 102 CB segments as in this article, but for

¹Paper No. JAWRA-12-0075-P of the *Journal of the American Water Resources Association* (JAWRA). Received March 27, 2012; accepted August 28, 2012. © 2013 American Water Resources Association. This article is a U.S. Government work and is in the public domain in the USA. **Discussions are open until six months from print publication.**

²Respectively, Senior Research Scientist (Wang), Virginia Institute of Marine Science, 410 Severn Avenue, Suite 109, Annapolis, Maryland 21403; Modeling Coordinator (Linker) and Associate Director for Science (Batiuk), Chesapeake Bay Program Office, U.S. Environmental Protection Agency, Annapolis, Maryland 21403 (E-Mail/Wang: pwang@chesapeakebay.net).

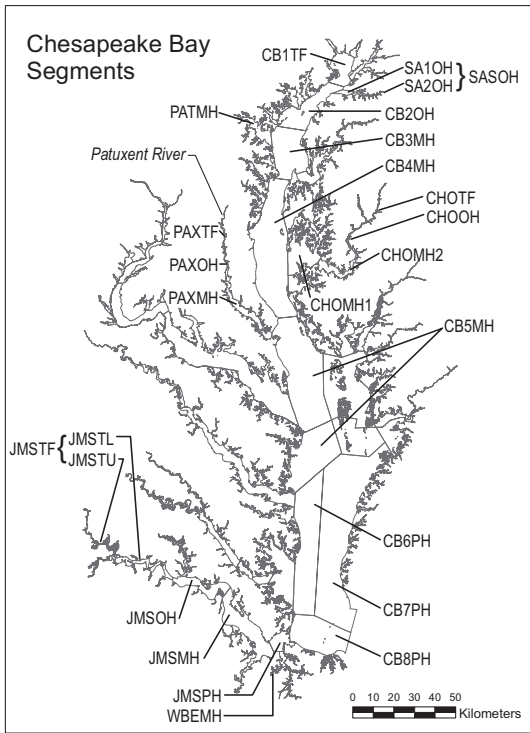


FIGURE 1. Chesapeake Bay (CB) Segments.

the TMDL the finer CB segmentation is aggregated up to the 92 TMDL CB segments. This article specifically addresses the SAV/water clarity standard and how a sediment allocation can be determined for any CB segment.

The Chesapeake water quality criteria are concentrations of DO, chlorophyll-*a* or K_d values that are protective of the Chesapeake living resources. Water quality standards are set by the states and are the application of water quality criteria at specific locations (designated uses) and times. The Chesapeake TMDL is aimed at full achievement of all the living resource-based water quality standards.

Submerged aquatic vegetation is an essential habitat in the CB, which provides food and shelter for juvenile crab and fish nurseries (Lubbers *et al.*, 1990; Orth and van Montfrans, 1990). It is estimated that Bay wide about 74,900 hectares of SAV are needed to ensure Bay living resources in a healthy condition (USEPA, 2003). However, the current SAV population is only about half the goal, due mainly to poor water clarity that inhibits light penetration (Kemp *et al.*, 1984, 2004).

Submerged aquatic vegetation in the Chesapeake estuary generally grows at depths of 2 m or less. In conditions of poor water clarity, light is absorbed or scattered in the path from the water surface to SAV leaves (Dennison *et al.*, 1993). To obtain a healthy SAV habitat, the CB Program set water clarity criteria within the 2-m depth contour in the tidal fresh and oligohaline regions, to have a minimum of 13%

light through water at specified depths (USEPA, 2003; Kemp *et al.*, 2004). The equivalent light through water for mesohaline and polyhaline regions which have SAV communities requiring higher minimum light levels is 22%.

Fractions of light (I/I_0) through a water column can be assumed follow the Lambert-Beer law (Jerlov, 1976; Kirk, 1983):

$$I = I_0 e^{-K_d Z}, \quad (1)$$

where K_d is diffused light attenuation coefficient (in m^{-1}) for water, and I_0 and I are light intensity at the water surface and at depth Z (in meters), respectively.

The CB Program, working closely with its seven watershed states, federal agencies, and the larger CB scientific community, derived and published CB water clarity criteria to establish the minimum level of light penetration required to support the survival, growth, and continued propagation of SAV (USEPA, 2003). CB-specific water clarity criteria were derived for low and higher salinity habitats using a worldwide literature synthesis, an evaluation of CB-specific field study findings, and application model simulations and diagnostic tools.

The water clarity criteria, applied only during the SAV growing seasons, were presented in terms of the percent ambient light at the water surface extending through the water column and the equivalent Secchi depth by application depth. The recommended percent light-through-water criteria can be directly measured using a Secchi disk or a light meter. A specific application depth is required to apply and determine attainment of the water clarity criteria.

Submerged aquatic vegetation restoration acreage criteria and water clarity application depths were developed based on historic and recent data on the distribution of SAV (USEPA, 2003). Detailed analyses using that data — including historical aerial photographs — were undertaken to map the distribution and depth of historical SAV beds in the CB and its tidal tributaries and embayments. The analyses led to the adoption of the single-best-year method that considers historical SAV distributions from the 1930s through the early 1970s and more recent distributions since 1978 to the present mapped through annual SAV aerial surveys of the Bay's shallow water habitats. Using that method, the U.S. Environmental Protection Agency and its watershed partners established a bay-wide SAV restoration criteria of 74,900 hectares based on Bay segment-specific SAV area criteria (USEPA, 2003).

In the CB TMDL, the water clarity criteria are specified to achieve the historically high area of SAV beds found in the CB. Water clarity criteria were set for the purpose of SAV recovery to achieve the CB

segment-specific SAV area goals (USEPA, 2007, 2010). The combined SAV restoration area/water clarity criteria for a CB segment is met if any of the following conditions are met: (1) the SAV area meets the CB segment's SAV restoration area criteria; (2) the area of shallow water that meets the water clarity criteria for the CB segment is at least 2.5 times the SAV restoration area criteria; or (3) combined SAV and water clarity areas meet the criteria. The combined area approach is applied when SAV area fails to meet the criteria. In that case, additional areas that meet the applicable water clarity criteria in the unvegetated shallow water area equal to 2.5 times the remaining SAV area, are added together to meet the criteria.

If there remains a deficit of SAV and water clarity area that meet the criteria in a CB segment, then sediment or nutrient reductions are required to achieve the water clarity standard in additional shallow areas of the segment. This article examines the case of when after assessing the SAV/clarity criteria it is found that further nutrient and sediment load reductions are needed.

Total suspended solids (TSS) and chlorophyll-*a* concentrations are of particular concern in the CB water clarity assessments (USEPA, 2003; Kemp *et al.*, 2004). Chlorophyll-*a* concentration is an extensively used index for eutrophication. It is sensitive to nutrient loads and has significant implications to DO depletion in the Chesapeake (Officer *et al.*, 1984). Nutrient control is key to attaining DO and chlorophyll-*a* water quality standards in the Chesapeake TMDL (USEPA, 2010).

Many nonpoint source management practices control both nutrients and sediment. Because bottom water DO in the mainstem of the Bay is the most stringent water quality standard in the CB, the reductions in nutrient and sediment loads to achieve the DO standard also achieve the SAV/clarity standard in most CB segments (USEPA, 2010). In those remaining cases where additional TSS and/or nutrient controls are required to achieve the SAV/clarity standards, tradeoffs between TSS and nutrient load reductions exist. To efficiently balance nutrient and sediment controls and to examine cost-effective management options to improve and maintain water clarity the relative sediment and nutrient effects on water clarity should first be elucidated.

Relationships between Kd, *in situ* TSS, and chlorophyll-*a* concentrations are an area of active research in the CB estuary (Gallegos, 2001; Kemp *et al.*, 2004; Gallegos *et al.*, 2005; Baldizar and Rybicki, 2006). This article draws and builds on the research and analyzes correlations of TSS and chlorophyll-*a* for all 102 CB segments, and further investigates the relative effects on Kd by TSS or chlorophyll-*a* in different salinity regimes and in different tributaries. Gallegos

(2001) developed a method to calculate required reductions in TSS and chlorophyll-*a* to improve water clarity to meet a target Kd. This article expands on that approach and links Kd to the watershed loads and analyzes the relationship of watershed nutrient and sediment loads with Kd, TSS, and chlorophyll-*a* in the estuarine water column to provide options for TMDL development and management implementation. This article also investigates sources of TSS loads and their relative effect on water clarity. Sources of TSS examined include loads from the ocean, resuspension in tidal waters, shore erosion, major river discharges to the Chesapeake, and from the Coastal Plain watershed excluding shore erosion.

Light Attenuation Assessment

The light attenuation coefficient, Kd, is dependent on the materials within the water column, including inorganic suspended solids (ISS), volatile or organic suspended solids (VSS), and dissolved organic matter (DOM) (Smith *et al.*, 1983; Stefan *et al.*, 1983; Gallegos, 2001). Light attenuation can be represented as:

$$Kd = Kd_0 + Kd_1 \text{ ISS} + Kd_2 \text{ VSS} + Kd_3 \text{ DOM}, \quad (2)$$

where Kd₀ is background attenuation of water, and Kd₁, Kd₂, and Kd₃ are the specific light attenuation coefficients for ISS, VSS, and DOM, respectively.

Usually DOM is included in the background light attenuation (k₀, due to water + DOM) (Cercio and Noel, 2004). Because chlorophyll-*a* and TSS (TSS = ISS + VSS) are routinely monitored throughout the study area, many researchers in the CB region have used the following equation (Gallegos, 2001; Kemp *et al.*, 2004) to assess Kd:

$$Kd = k_0 + k_1 \text{ TSS} + k_2 \text{ Chl} \quad (3)$$

Although Kd, based on PAR (photosynthetically active radiation), has been measured in many of the more than 150 CB tidal water quality monitoring program stations in recent years, Secchi depth has been measured at all stations routinely throughout the 29-year history of the CB monitoring program. Secchi depth was converted to Kd based on the approximation of Kd = 1.45/Secchi depth (USEPA, 2003).

METHODS

A combination of monitoring data and model scenario-based outputs were used in the assessment.

The models were a watershed model and an estuarine water quality model of the Chesapeake.

The watershed nonpoint N, phosphorus (P), and sediment loads used in the analysis are based on the CB Watershed Model, version 5.3 (Shenk and Linker, this issue). The watershed model uses the Hydrodynamic Simulation Program — Fortran software (Bicknell *et al.*, 1997) that simulates hourly processes in more than 1,000 land-river segments in the watershed, and provides daily flow, nutrient, and sediment loads to an estuarine simulation of the Bay called the Water Quality and Sediment Transport Model (WQSTM) (Cercio *et al.*, 2010). The Watershed Model was calibrated with 1985-2005 observed data, and had about a 0.95 model efficiency (Nash and Sutcliffe, 1970) on loads at major river tributaries. Point source loads, including loads discharged directly to tidal waters, were directly reported by the 473 significant wastewater discharging facilities.

The estuarine water quality model is a coupled CH3D Hydrodynamic Model (HM) and the integrated computational water quality model (ICM) of the Chesapeake called the WQSTM (Cercio *et al.*, 2010; Cercio and Noel, this issue; Cercio *et al.*, this issue). The WQSTM grid consists of 56,920 model cells with average cell dimensions of about 1 km × 1 km × 1.5 m depth. The HM simulates estuarine circulation in a 90-s time interval, and derives current, wind-induced wave, shear stresses, salinity, and temperature distributions that provide forcing for the water quality model. The WQSTM receives daily nutrient and sediment loads from the Watershed Model and simulates 36 state variables including the various species of N, P, carbon, silica, DO, salinity, temperature, three types of algae, two types of zooplankton, oysters, menhaden, SAV, and inorganic solids (clay, silt, and sand). The model deals with hundreds of differential equations to simulate physical, chemical, and biological reactions (Cercio and Noel, 2004; Cercio *et al.*, 2010) including algal processes, sediment transport, and water clarity. The Kd simulation is based on the Gallegos *et al.* (2011) optical model, which accounts the effects from chlorophyll-*a*, TSS, DOM, and seasonal factors. The coupled estuarine hydrodynamic, water quality, and sediment transport models were calibrated for the years 1993-2000, and verified to be acceptable for a simulation period of 1985-2005. The mean error of chlorophyll-*a* is -0.32 µg/l in the mainstem Bay, and around -1.5 µg/l in the tributaries; the mean error of light attenuation is 0.065 1/m in the mainstem Bay, and from 0.1 to 0.135 1/m in the tributaries.

Analysis Using Observed Water Quality Data

Relationship of Observed Kd with Observed In Situ Chlorophyll-*a* and TSS. Correlation

analysis was used to study the effect on Kd by TSS and chlorophyll-*a* on a CB segment basis. Observed Kd, TSS, and chlorophyll-*a* data were assembled from about 200 stations in the estuary from 1985 through 2009, and aggregated to monthly data for the 102 CB segments. According to Equation (1), the allowable maximum Kd (labeled allowable Kd_max) for a CB segment that meets the minimum requirement for SAV growth can be determined from the required percent light through water (*I/I₀*) and the specified application depth (*Z*):

$$Kd_{max} = \frac{-\ln(I/I_0)}{Z} \tag{4}$$

The CB segment-specific minimum light requirements for specified depths applied to SAV, i.e., the application depth, were originally published by Batiuk *et al.* (2000).

From Equations (4) and (3), Gallegos (2001) estimated a linear proportion of the relationship between TSS and chlorophyll-*a* for an allowable maximum as Kd:

$$TSS = \frac{-\ln(I/I_0)/Z - k_0}{k_1} - \frac{k_2}{k_1} Chl \tag{5}$$

Equation (5) defines a line with slope = -k₂/k₁, and chlorophyll-*a* = 0 intercept of (-ln(*I/I₀*)/*Z* - k₀)/k₁ in the TSS vs. chlorophyll-*a* plot (Figure 2). The pair of TSS and chlorophyll-*a* concentrations on the dotted line yields allowable Kd_max, the allowable maximum Kd. The TSS and chlorophyll-*a* concentrations in the area from the dotted line to the origin have Kd complying with the requirement. Otherwise, in the case of Kd > allowable Kd_max as denoted in the case of the star symbol in Figure 2, reductions in TSS and/or chlorophyll-*a* concentrations would be needed

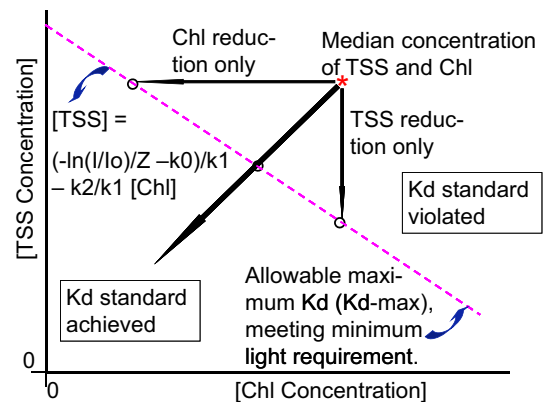


FIGURE 2. Estimating the Required Total Suspended Solids (TSS) and Chlorophyll-*a* Concentrations in Water to Reach a Target Kd (modified from Gallegos, 2001).

in the CB segment to achieve the minimum light requirement (Gallegos, 2001).

Relationship of Observed TSS and Chlorophyll-*a* in Water with Model Estimated Watershed Loads. Once a required reduction in TSS and chlorophyll-*a* concentrations in the water column using the preceding analysis is determined to be needed, the question arises as to how to most effectively achieve the required reductions by further reducing nutrient and/or sediment loads from the watershed. A correlation analysis was conducted on TSS and chlorophyll-*a* concentrations in tidal waters with local watershed sediment and nutrient loads for the CB segments. The local loads for a tidal water CB segment are those from the adjacent watershed including any major river discharge into the CB segment. The derived correlation approximates the correlation of *K_d* with the effective load on the CB segment if the impact on the segment by the load from other areas can be shown to be small or can be proportionally approximated through additional analysis.

In a correlation analysis developed in this article (later illustrated in Figure 5), yearly and monthly averaged values of loads over the 1985-2005 period were used. The so-called “algal unit,” defined as 1 unit mass of P or total phosphorus (TP) and 10 units mass of (N) or total nitrogen (TN) (Koroncai *et al.*, 2003), has been used to normalize nutrient load to assess the combined N and P nutrients’ effect on eutrophication. This assumes nutrients are taken up by algae in roughly a 10:1 N:P ratio (by weight), approximating a Redfield 7:1 weight/weight ratio. The 10:1 weight ratio of nitrogen to P used in this article is informed by both the Redfield ratio of 7.2:1 (i.e., 16:1 for stoichiometric N:P) (Redfield *et al.*, 1966) and the TMDL load ratio of nitrogen to P of about 15:1. Accordingly, this article uses $(TN + 10 TP)/2$ to represent the combined TN and TP load effects, referring to it as the weighted nutrient load (WNL). Under existing conditions, the annual average TN load to the Bay is about 8-15 times the annual average TP load to the Bay from the major tributaries.

Relationship of Observed *K_d* with Model Estimated Watershed Loads. The correlations of observed *K_d* with model estimated local sediment and nutrient loads for each CB segment were also analyzed.

Analysis Using Estuarine Water Quality and Sediment Transport Model for Clarity Assessment

Similar to the correlation analyses using observed *K_d*, TSS, and chlorophyll-*a* in the preceding sections, the corresponding correlations using model simulated

K_d, TSS, and chlorophyll-*a* were also analyzed. The purpose was to compare the counterpart results to check the validity of using the model. The following three aspects of models were used to provide information that cannot be accomplished using observed data alone.

Set of Sensitivity Scenarios with Differential Nutrient and Sediment Loads. This analysis used a set of four model scenarios, which had different nutrient (TN and TP) *vs.* sediment loads (Table 1) to analyze relative importance of nutrient and sediment on CB segment water clarity. All four scenarios were simulated for a 10-year period using a 1991-2000 hydrology.

Analysis of *K_d* Sensitivity to Different Sediment Sources. This analysis used a set of sediment scoping scenarios, to estimate the sensitivity of *K_d* in the CB segments to five key sediment sources. The five sediment sources were ocean sediment loads, resuspended sediment loads in shallow tidal waters, shoreline erosion sediment loads, riverine sediment loads from the major rivers, and sediment loads from the entire watershed. This was done by turning off a single key sediment source from the base scenario to analyze the relative importance of each sediment source on water clarity.

- (A) *Base Scenario*: Year 2010 Tributary Strategy Scenario (Shenk and Linker, this issue), which includes all sediment source types;
- (B) *No Ocean Sediment*;
- (C) *No Bed Resuspension*;
- (D) *No Shore Erosion Sediment*;
- (E) *No Major River Sediment*;
- (F) *No Watershed Sediment* (both major river sources and coastal plain loads).

Scenarios B through F were compared against the Scenario A (*Base Scenario* load) to calculate simulated *K_d* sensitivity, and the effect of different sediment source types on *K_d*.

Geographically Isolated Sediment Loading Sources. This analysis used a set of sensitivity loading scenarios by removing sediment loads from a specific geographic area to analyze the relative effects of sediment loads from different geographic areas on water clarity in individual model cells or CB segments. Using the tidal Patuxent River as an example (Figure 3), the tidal reach was divided into four regions (Regions 2, 3, 4, and 5). Region 1 was assigned to the nontidal free-flowing portion of the Patuxent River in the watershed and Region 6 was assigned to the sediment loads of all the rest of the

TABLE 1. Nutrient and Sediment (Sed) Loads in the Set of Four Model Sensitivity Scenarios.

Scenario	Units of Nutrient Load	Sed Load	Note
A	WNL = 291 (TN = 342, TP = 24.1)	9,780 Units	1985 condition
B	WNL = 165 (TN = 187, TP = 12.5)	6,042 Units	46.4% WNL reduction and 38.2% Sed reduction from 1985 condition
C	WNL = 165 (TN = 187, TP = 12.5)	9,780 Units	46.4% WNL reduction from the 1985 condition
D	WNL = 291 (TN = 342, TP = 24.1)	6,042 Units	38.2% Sed reduction from the 1985 condition

Notes: One load unit is equivalent to 453,600 kg/yr. WNL, weighted nutrient load; TN, total nitrogen; TP, total phosphorus.

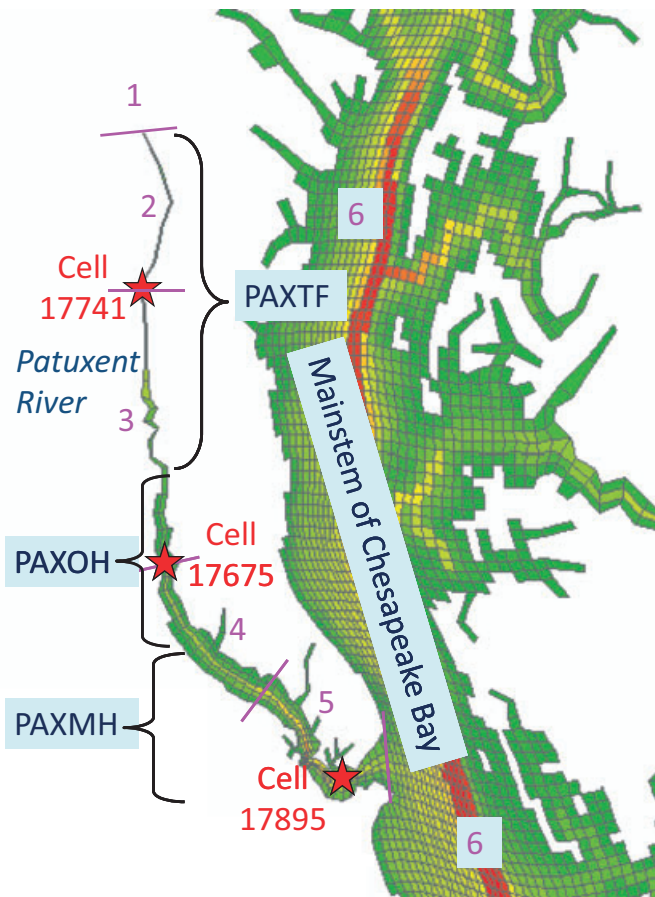


FIGURE 3. Six Source Regions in the Patuxent Sediment Geographic Loading Scenarios.

CB watershed other than the Patuxent. The set of seven scenarios that were run are as follows:

- (A) Base scenario;
- (B) No sediment load from Region 1;
- (C) No sediment load from Region 2;
- (D) No sediment load from Region 3;
- (E) No sediment load from Region 4;
- (F) No sediment load from Region 5;
- (G) No sediment load from Region 6.

The base scenario has daily sediment and nutrient loads from all six regions. All scenarios were run using 2003-2005 hydrology and loads and the CB

Water Quality Sediment Transport model generated average sediment concentrations in specific model cells were used. The effect of sediment from a region, Region 2 for example, on a specific cell can be derived from the difference of sediments in the cell between the base scenario and Scenario C. The combined effect of sediment loads from multiple regions on a specific cell or cell groups can also be calculated.

RESULTS AND DISCUSSION

Analysis Using Observed Water Quality Data

Correlation analysis was used on the observed data. The correlations have a significance level at $p = 0.05$. The discussion emphasizes the strength of the correlation between K_d and TSS concentrations, called the “correlation coefficient of TSS,” and the correlation between K_d and chlorophyll-*a* concentrations, called the “correlation coefficient of chlorophyll-*a*.”

Relationship of Observed K_d with Observed *In Situ* Chlorophyll-*a* and TSS. Figure 4 plots the correlation coefficients of observed chlorophyll-*a* and TSS for the 102 CB segments. The CB Program uses a two-character suffix to distinguish different salinity regimes in the segment names: TF for tidal fresh, OH for oligohaline, MH for mesohaline, and PH for polyhaline (USEPA, 2004). Generally, the chlorophyll-*a* and TSS correlation coefficients in tidal fresh and oligohaline CB segments behave in a similar manner.

In most tidal fresh and oligohaline CB segments, correlation coefficients of TSS are greater than the correlation coefficients of chlorophyll-*a*, and in some cases CB segments have negative chlorophyll-*a* correlation coefficients. The negative correlation between chlorophyll-*a* and K_d can be related to the higher light attenuation by TSS that, in turn, limits algal growth. Also, TSS is a super component, which consists of ISS and VSS (VSS includes algal particles). In cases of a strong correlation between K_d and TSS,

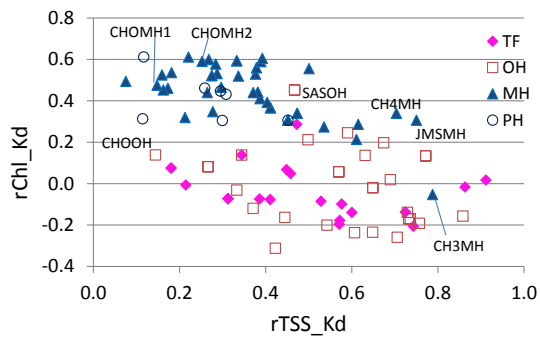


FIGURE 4. Correlation of Observed K_d with *In Situ* Total Suspended Solids (TSS) (denoted as r_{TSS_Kd}) or Chlorophyll- a (denoted as r_{Chl_Kd}).

if the major component of TSS that affects K_d is ISS (rather than chlorophyll- a) and the variation in ISS is not concordant with the chlorophyll- a variation, weak or negative correlations between chlorophyll- a and K_d can result despite chlorophyll- a still being a contributor to K_d .

In contrast to the tidal fresh and oligohaline CB segments, in most mesohaline and polyhaline CB segments, correlation coefficients of chlorophyll- a are greater than zero and are slightly greater than correlation coefficients of TSS, indicating that chlorophyll- a is usually the dominant influence on K_d in the mesohaline and polyhaline segments.

Another approach to examine the influence of TSS or chlorophyll on K_d is to calculate the following ratio and denote it as R_{cs} :

$$R_{cs} = (r_{TSS} + r_{Chl})/r_{TSS},$$

where r_{TSS} is the correlation coefficient between K_d and TSS, r_{Chl} is the correlation coefficient between K_d and chlorophyll- a .

The greater the R_{cs} is, the more contribution from chlorophyll- a to light attenuation, or conversely the less contribution from TSS on K_d . Of the 50 CB segments with $R_{cs} < 1.45$ 47 are tidal fresh or oligohaline, except for the CB segments of CB3MH, CB4MH, and JMSMH. The 35 CB segments with $R_{cs} > 2.0$ are all mesohaline or polyhaline segments. The 17 CB segments with R_{cs} between 1.45 and 2.0 involve all four salinity regimes and can be regarded as a transitional cluster.

The discharge point of the free-flowing rivers into the Chesapeake tidal waters can be a major source of sediment load. Tidal fresh and oligohaline CB segments are closer to the point of river discharge, therefore, they are affected more than the mesohaline and polyhaline CB segments. Sediment in the estuary is also affected by resuspension and other sources such as shore erosion. In the aforementioned

47 tidal fresh and oligohaline CB segments, the resuspension and shore erosion sources affect K_d less significantly than the major river discharge source. In the case of CB3MH, it is close to the Bay's turbidity maximum, which varies in the region of CB2OH to CB3MH depending on Susquehanna River flow. Within the region of the turbidity maximum sediment still plays a greater role on influencing K_d than chlorophyll- a does, showing higher correlation coefficients of TSS and lower correlation coefficients of chlorophyll- a than more saline CB segments (Figure 4). In contrast in CB4MH, which is farther away from CB2OH, the effect of sediment on K_d becomes weaker.

Besides the distinction among salinity regimes, local conditions or tributary characteristics can also cause a cluster of CB segments to have distinct sediment *vs.* chlorophyll- a effect on K_d . In the James River, JMSMH has a relatively low R_{cs} ($=1.35$), and the R_{cs} of JMSPH is still relatively low (2.02, nearly in the transitional cluster's R_{cs} ranges of 1.45-2.0), as well as a relatively higher correlation coefficient of TSS than most saline CB segments. The James tidal fresh (JMSTF) and oligohaline (JMSOH) also have lower R_{cs} , at 0.72 and 0.93, respectively. The tidal James River K_d is generally more sensitive to TSS than chlorophyll- a .

Another example of distinct tributaries in sediment *vs.* chlorophyll- a effect on K_d , but in the opposite direction, is the Choptank River. The R_{cs} ($=1.96$) in CHOOH is higher than most tidal fresh and oligohaline and even higher than some mesohaline CB segments in the transitional cluster. This can be partly explained by the relatively higher salinity (5.4 ppt) in CHOOH than in most oligohaline CB segments. Consistent with the higher salinity, CHOMH1 and CHOMH2 have a relatively high chlorophyll- a effect on K_d ($R_{cs} > 3.0$). The R_{cs} in SA1OH and SA2OH (combined as SASOH with average salinity of about 0.6 ppt) of the Sassafras River equals 1.97, which is due to relatively high correlation coefficients of chlorophyll- a ($=0.45$) besides moderately high correlation coefficients of TSS ($=0.47$) (Figure 4).

In contrast to the low salinity regimes, in the 35 mesohaline and polyhaline CB segments (having $R_{cs} > 2.0$) the sediment influence on K_d was weaker. In mesohaline and polyhaline CB segments, most sediment from major river discharges has settled before transport to these segments, while other source types of sediment, i.e., resuspension or shore erosion, may be low, causing chlorophyll to be a greater contributor to K_d . In tidal fresh and oligohaline CB segments, the sediment contribution to K_d is more important. In general, the differences in sediment *vs.* chlorophyll- a effects on K_d among tributaries are less

significant than their differences among salinity regimes.

A limitation of this approach is that TSS includes ISS and VSS and that VSS is primarily algae (chlorophyll-*a*). Chlorophyll-*a* is different from ISS, and chlorophyll-*a* has distinct light absorption characteristics (Gallegos and Bergstrom, 2005). Therefore, the correlation coefficients of TSS and rChl values are only indirectly comparable. Likewise the Rcs values are meaningful only in the comparison of their relative values to get a sense of the relative importance of TSS and chlorophyll-*a* on Kd. Another limitation of this approach is that the inorganic solids consist of sand, silt, and clay. For the same amount of ISS load a higher Kd will result if the ISS consists primarily of finer particles. The influences on Rcs by different sand, silt, and clay sediment components cannot be assessed due to limited observations of the sediment composition measurements at the long-term water quality monitoring stations.

Relationship of Observed TSS and Chlorophyll-*a* in Water with Model Estimated Watershed Loads. Figure 5 plots correlation coefficients of model estimated sediment load with TSS concentrations (i.e., rSed_TSS), and the coefficients of the WNL with chlorophyll-*a* concentrations (i.e., rWNL_Ch1) for the four salinity regimes. Similar to Figure 4, Figure 5 shows a distinct cluster of tidal fresh and oligohaline CB segments from the mesohaline and polyhaline CB segments. Most mesohaline and polyhaline CB segments have greater rWNL than the tidal fresh and oligohaline CB segments, and the correlation of chlorophyll-*a* with nutrient load is stronger than the correlation of TSS with sediment load. This is partly related to a longer residence time of nutrients in the more saline CB segments due to the estuarine circulation. The negative rWNL_ch1 (=−0.45) and moderately high rSed_TSS (=0.31) in CB3MH may be due to the reason discussed in the preceding section that resuspension in the turbidity maximum region may cause CB3MH to be affected more by sediment than by chlorophyll-*a*. In tidal fresh and oligohaline CB segments, the correlations of TSS with sediment load are stronger than the correlation of chlorophyll-*a* with nutrient load. The comparability between Figures 5 and 4 indicates that local loads have significant impact on light attenuation.

Low rSed and rWNL values mean there are sources other than the watershed loads, such as shore erosion, resuspension, or supply from other CB segments that are influencing Kd. Seasonal changes and lag time in the response of TSS and chlorophyll-*a* in water to the loads could also play a role.

When the estuary is analyzed as a whole unit responding to annual sediment and nutrient loads

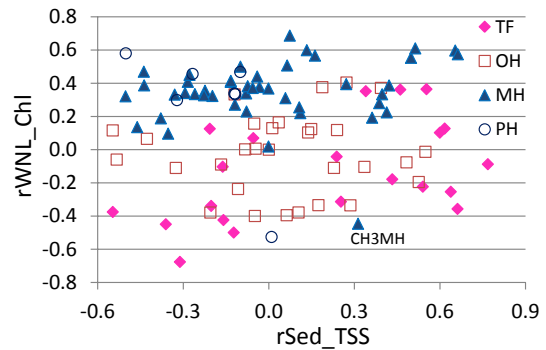


FIGURE 5. Correlation of Total Suspended Solids (TSS) with Sediment Load (denoted as rSed_TSS), Chlorophyll-*a* with Weighted Nutrient Load (WNL) (denoted as rWNL_ch1).

into the whole Bay, we observed monotonic changes of TSS, chlorophyll-*a*, or Kd with the change in nutrient and sediment loads (Wang *et al.*, 2002), but analysis at the CB segment level using monthly data, reveals a more complicated relationship.

Relationship of Observed Kd with Model Estimated Watershed Loads. The correlations of observed Kd with sediment load (rSed_Kd) and WNL (rWNL_Kd) were analyzed. Most CB segments have positive rSed_Kd and rWNL_Kd. In many cases, if rSed_Kd is higher (>0.35), rWNL_Kd is also higher (>0.2), especially for tidal fresh or oligohaline CB segments. The CB segments with high rSed_Kd are generally tidal fresh or oligohaline although some CB segments have negative rSed_Kd and/or negative rWNL_Kd.

Kd is principally governed by TSS and chlorophyll-*a* in the water column. The TSS and chlorophyll-*a* concentrations are affected by sediment and nutrient loads, however, some CB segments, especially the more saline CB segments, lack a direct correlation between Kd and sediment and nutrient loads, indicating that complex processes have occurred between the loading sediment and nutrients and their ultimate influence on CB segment Kd. Seasonal variation and the lag time of water quality response to loading materials may be implicated. The tidal fresh and oligohaline CB segments have shorter lag times, and show more correlation with watershed load.

Analysis Using Estuarine Water Quality and Sediment Transport Model for Clarity Assessment

The correlation analyses using modeled Kd, TSS, and chlorophyll-*a* yield similar results as those using observed Kd, TSS, and chlorophyll-*a* in the preceding sections, providing confidence in using model results. The following are additional analyses using modeled results.

Implications of the Results from Model Scenario Set with Differential Nutrient and Sediment Loads. From the differential loading scenarios (Table 1) we get WQSTM estimated K_d from the four scenarios: K_{dA} , K_{dB} , K_{dC} , and K_{dD} (Table 2). The scenario K_{dB} is the scenario of reduction in both sediment and nutrients, which has the lowest K_d among the four scenarios. K_{dA} is the base scenario of highest loads in both sediment and nutrient, which has the highest K_d . Generally, $K_{dA} > (K_{dC} \text{ or } K_{dD}) > K_{dB}$. We calculated K_d differences between pair scenarios: $dKs1 = K_{dA} - K_{dD}$, $dKs2 = K_{dC} - K_{dB}$, $dKn1 = K_{dA} - K_{dC}$, and $dKn2 = K_{dD} - K_{dB}$.

The $dKs1$ and $dKs2$ are K_d improvements through sediment (Sed) load reduction under WNL levels at 291 and 165 units, respectively. The $dKn1$ and $dKn2$ are K_d improvements through nutrient reduction, under sediment load levels at 9,780 and 6,042 units, respectively. In most CB segments, $dKs1$ are slightly greater than $dKs2$. This indicates that K_d improvement through TSS load reduction in different nutrient loading levels are similar, and more effective in higher nutrient loads. Similarly, in most CB segments, $dKn1$ are slightly greater than $dKn2$, indicating that K_d improvement through nutrient load reduction in different sediment loading levels are similar, and more effective in higher sediment levels. The fresher water CB segments generally have higher dKs than more saline CB segments, suggesting that sediment load reduction improves K_d more effectively for tidal fresh and oligohaline CB segments. Most saline CB segments and some fresher water segments have relatively high dKn , suggesting reduction in nutrient load can effectively improve K_d in these segments.

A limitation of this approach is that the scenarios are based on basin-wide load changes. If the differential sediment and nutrient load scenarios were based on local load variations (i.e., other sources kept unchanged), the simulated influence on K_d by nutrient load change (*vs.* by sediment load change) would become less prominent. This is because under basin-wide load change, the involved CB segment can also be impacted by the load change in other sources, while dissolved inorganic nutrients and algae can transport relatively more widely than sediment in a certain time period impacting the involved CB segment.

The last column of Table 2 is: $Rs/n = dKs1 / (dKs1 + dKn1)$, and the table is sorted by Rs/n in descending order. Rs/n represents relative importance of sediment reduction *vs.* nutrient reduction on K_d improvement. Rs/n values range from 0 to 1. The closer to 1 the Rs/n is, the greater influences of K_d by sediment load. The closer to 0 the Rs/n is, the greater influences of K_d by nutrient load. The CB segments with $Rs/n > 0.2$ are generally tidal fresh and oligohaline where sediment contributes to K_d significantly.

Most mesohaline and polyhaline CB segments have low Rs/n (< 0.2 , with $dKs2 < 0.1$). There, nutrient contributions to K_d are significant; or alternatively, chlorophyll-*a* contributions to K_d are significant, because chlorophyll-*a* levels are generally related to nutrient load. The results from this analysis are consistent with what is drawn from the monitoring data analysis.

Some CB segments, which are exceptions to the above finding, were found to have higher Rs/n in mesohaline or polyhaline CB segments, or lower Rs/n in the tidal fresh or oligohaline CB segments. The JMSMH and JMSPH have $Rs/n = 0.41$ and 0.24 , respectively. Other mesohaline CB segments in the James River such as WBEMH (with $Rs/n = 0.27$) also display similar results. This suggests that the contribution of sediment to K_d is relatively more important in the tidal James River than in many other tidal tributaries. This phenomenon is consistent with what was derived from the monitoring data analysis in the James River above. CHOOH and CHOTF have relatively lower Rs/n , 0.03 and 0.16 , respectively, suggesting the relative importance of nutrient effect on K_d in tidal fresh and oligohaline of the tidal Choptank River than in many other tidal fresh or oligohaline CB segments. This conclusion is also consistent with what we derived from Figure 4 on the tidal Choptank River based on the observed data.

Method to Estimate Sediment and Nutrient Load Reduction to Achieve Target K_d . The x and y axes in Figure 6 are WNL and sediment (Sed) loads, respectively. Based on WNL and Sed loads, the four scenarios (A, B, C, and D) can be located, as the four circles. Using JMSTFU as an example, the values by the circle are corresponding K_d of the four scenarios, K_{dA} , K_{dB} , K_{dC} , and K_{dD} (referring to Table 2). We then draw K_d isopleths as function of percent Sed and WNL loads. Assuming in the current condition in JMSTFU, K_d is 2.3, and the WNL load is 80% the 1985-reference level as the star sign in Figure 6. Like many tidal fresh CB segments, the K_d isopleths are relatively flat because of more significant effect on K_d by sediment than by nutrients. For $f = I/I_0 = 13\%$ light through water at $Z = 1$ m (application depth), it requires $K_d \leq 2.04$. This can be achieved by either reducing sediment load only as arrow RA, or combined reducing sediment load (RBs) and nutrient load (RBn), e.g., arrow RB. The percent reduction in Sed and WNL loads can then be estimated from the plot.

If the modeled K_d is calibrated perfectly, we can use the observed K_d as the current K_d in the above analysis. Otherwise, it is better to use the model simulated current K_d . If all measurements and model go ideally, the lines of current Sed load and WNL load will meet on the K_d isopleths of current condition.

TABLE 2. Simulated Kd (in 1 m^{-1}) in Differential TSS and Nutrient Load Scenarios.

CB Segment	KdA	KdB	KdC	KdD	Rs/n	CB Segment	KdA	KdB	KdC	KdD	Rs/n
JMSTFU	2.75	1.95	2.65	2.05	0.88	PO2OH	1.85	0.83	0.86	1.69	0.14
APPTF	2.50	1.85	2.27	2.05	0.66	DENTF	2.04	1.81	1.85	2.01	0.13
DCPTF	2.88	2.04	2.53	2.39	0.59	CB4MH	1.72	1.06	1.12	1.63	0.13
JMSTFL	2.78	1.73	2.26	2.14	0.55	OCEAN	0.90	0.80	0.81	0.89	0.12
C12TF	2.59	1.73	2.13	2.13	0.50	POMMH	1.27	0.78	0.80	1.21	0.12
JMSOH	3.93	2.17	2.91	2.93	0.50	MATTF	2.24	1.49	1.56	2.15	0.12
POCTF	2.37	1.72	2.01	2.08	0.45	SOUMH	2.82	1.17	1.24	2.62	0.11
C11TF	2.65	1.64	2.01	2.17	0.43	RHDMH	2.24	1.02	1.08	2.10	0.11
PMKTF	2.80	1.57	2.00	2.22	0.42	SEVMH	1.75	0.93	0.97	1.66	0.11
JMSMH	3.27	1.89	2.36	2.63	0.41	CMDOH	1.11	0.81	0.83	1.08	0.10
PAXTF	3.55	2.34	2.76	3.03	0.40	RPPMH	2.12	1.15	1.21	2.02	0.10
MDPTF	2.58	1.66	1.97	2.18	0.39	MDNTF	4.26	2.80	2.89	4.12	0.09
CB2OH	3.20	1.81	2.21	2.60	0.38	VPCMH	1.74	0.68	0.72	1.64	0.09
MPNTF	1.07	0.77	0.86	0.94	0.38	MPCMH	1.83	0.68	0.73	1.72	0.09
PISTF	1.66	1.29	1.41	1.51	0.37	POVMH	1.09	0.65	0.66	1.06	0.08
RPPTF	2.92	2.20	2.44	2.64	0.37	YRKP	1.44	0.77	0.79	1.38	0.08
PMKOH	3.26	1.71	2.02	2.63	0.34	PA1MH	1.15	0.60	0.61	1.11	0.08
MPNOH	1.55	1.08	1.19	1.37	0.33	PA4MH	1.28	0.54	0.55	1.22	0.08
GU1OH	2.53	1.38	1.62	2.09	0.33	CDDOH	1.05	0.80	0.82	1.03	0.08
BACOH	3.29	2.67	2.84	3.07	0.33	EBEMH	1.97	1.36	1.39	1.92	0.07
SA1OH	3.05	1.77	2.07	2.59	0.32	CHSTF	2.46	1.71	1.76	2.41	0.06
GU2OH	1.85	1.09	1.27	1.58	0.32	CHSMH	1.05	0.63	0.64	1.02	0.06
BSHOH	2.36	1.39	1.56	2.04	0.28	CHOMH1	1.16	0.57	0.58	1.12	0.06
PAXOH	2.26	1.38	1.56	1.99	0.28	WSTMH	1.10	0.47	0.48	1.06	0.06
MPCOH	3.77	2.15	2.59	3.30	0.28	PA3MH	0.96	0.60	0.61	0.94	0.06
PATMH	2.67	1.75	1.95	2.39	0.28	NANOH	5.08	2.97	3.00	4.95	0.06
POVTF	2.30	1.45	1.63	2.04	0.28	MD5MH	1.34	0.76	0.77	1.31	0.06
WBEMH	1.58	1.15	1.26	1.46	0.27	CHSOH	1.25	0.99	1.00	1.24	0.06
CB3MH	2.19	1.28	1.45	1.91	0.27	EASMH	0.85	0.47	0.47	0.83	0.05
CHKOH	3.09	1.01	1.17	2.42	0.26	CB7PH	1.03	0.58	0.58	1.01	0.05
EL1OH	1.83	1.13	1.25	1.63	0.26	VA5MH	1.03	0.51	0.51	1.01	0.04
MIDOH	2.53	1.39	1.55	2.19	0.26	WICMH	3.37	2.06	2.07	3.31	0.04
EL2OH	1.34	1.02	1.09	1.26	0.25	NANMH	3.42	2.00	2.02	3.36	0.04
PO1OH	2.95	1.37	1.58	2.51	0.24	LCHMH	1.32	0.59	0.59	1.29	0.04
JMSPH	1.64	1.02	1.11	1.48	0.24	CB6PH	1.16	0.63	0.64	1.14	0.04
NORTF	4.17	2.34	2.59	3.70	0.23	MOBPH	1.10	0.58	0.58	1.08	0.04
MAGMH	2.51	1.51	1.67	2.27	0.22	TAVMH	1.11	0.57	0.58	1.09	0.04
ELIPH	1.58	1.13	1.20	1.47	0.22	SA2OH	1.76	1.21	1.23	1.73	0.04
RPPOH	2.90	1.90	2.05	2.66	0.22	CHOOH	1.83	1.27	1.29	1.81	0.03
VPCOH	4.19	2.18	2.57	3.74	0.22	TA2MH	2.22	0.92	0.92	2.18	0.03
POVOH	2.36	1.18	1.32	2.08	0.21	HNGMH	1.92	0.59	0.59	1.88	0.03
YRKM	2.48	1.45	1.60	2.26	0.20	TA1MH	1.32	0.58	0.58	1.30	0.03
BOHOH	2.40	1.46	1.56	2.20	0.19	PIAMH	1.25	0.48	0.49	1.24	0.02
MDATF	3.50	2.59	2.76	3.33	0.19	CHOMH2	1.39	0.73	0.73	1.38	0.02
PA2MH	1.46	0.64	0.69	1.29	0.18	BI1MH	1.96	0.56	0.56	1.94	0.01
SBEMH	2.00	1.52	1.60	1.92	0.17	CRRMH	1.52	0.56	0.56	1.52	0.01
LAFMH	1.34	0.96	1.00	1.27	0.16	BI2MH	3.00	1.10	1.10	3.00	0.00
CB8PH	0.91	0.68	0.70	0.87	0.16	FSBMH	7.15	4.48	4.48	7.15	0.00
CHOTF	1.25	0.91	0.97	1.19	0.16	MA1MH	1.98	0.60	0.60	1.98	0.00
DCATF	2.42	1.52	1.66	2.28	0.15	MA2MH	2.69	1.32	1.32	2.69	0.00
PO3OH	1.76	0.73	0.75	1.60	0.14	PA5MH	1.85	1.48	1.51	1.85	0.00

Note: TSS, total suspended solids; CB, Chesapeake Bay.

However, they can fail to meet at a point due to model uncertainty or measurement errors. Thus, using one of the loading components to draw a line to meet the current Kd isopleths, preferably the one yielding a higher angle intersection is recommended. More scenarios may be designed to increase accuracy on the above estimates.

In the above analysis, the loads are baywide, summed from all distributed sources. Figure 6 is applicable to the bay-wide management that paid similar efforts to reduce nutrient and sediment load from the major basins as the past management practice (CEC, 2000). Significant efforts have been made in the CB management by reducing nutrient and sed-

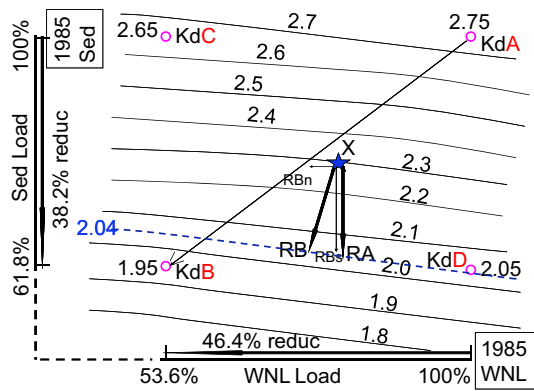


FIGURE 6. Illustration of Estimating Sediment and Nutrient Load Reduction to Reach a Target Kd.

iment load to improve DO water quality, especially focusing summer DO in deep waters since deep water DO is the most stringent water quality standard in the CB. Under these loading-reduction efforts, the water clarity in most CB segments is likely to meet or close to meet their standards. If some CB segments can still not meet the water clarity standard, further reduction in nutrient and sediment load is needed from the bay-wide control, then the above analyses using bay-wide load are applicable. However, this study shows that the loads, especially sediment load, from local watershed affects water clarity significantly. If we want to improve water clarity cost-effectively, we then control nutrient and sediment locally. We can construct a plot similar to Figure 6, but using localized WNL and Sed load to make suggestions on load control from the most influencing sources. The next two sections will further discuss modeling efforts on water clarity assessment.

Analysis of Kd Sensitivity to Different Sediment Sources. Eleven CB segments from the mainstem Bay and the Patuxent tributary are represented in Tables 3-5. The tables show the absolute values and the percent change estimated in Kd, TSS, and ISS in the source-sensitivity scenarios compared to the *Base Scenario*.

The big decreases in Kd in the *No Bed Resuspension* scenario indicates that resuspension plays an important role in light attenuation. The CB segment CB2OH is influenced the greatest by resuspension, because CB2OH is in the region of the Bay's estuarine turbidity maxima. Resuspension is relatively less important for Kd in tidal fresh CB1TF, because the major river sediment sources are the dominant influences, as can be seen from the relatively large changes of Kd in CB1TF in the *No Major River Sediment* scenario. Both CB1TF and CB2OH are close to the discharge point of Susquehanna River, and both are influenced signifi-

cantly by its sediment load. The watershed nonpoint source (NPS) sediment loads (including sediment from major rivers and the Coastal Plain watershed adjacent to the tidal Bay) is also important, as can be seen from the significant changes in Kd in most mainstem CB segments in the *No Watershed Sediment* scenario.

Segments CB8PH, CB7PH, and CB6PH are close to the CB mouth and the ocean sediment source influences them significantly, as can be seen from the relatively higher percent reduction in Kd in the *No Ocean Sediment* scenario.

Shoreline erosion also supplies sediment to the Chesapeake tidal waters with shore erosion loads equivalent to sediment loads from the watershed. The CB segments CB2OH, CB4MH, and CB5MH have relatively more shoreline and the WQSTM cells representing these CB segments have greater shore erosion loads. These CB segments also have greater Kd reductions in the *No Shore Erosion Sediment* scenario. The table values suggest that although sediment from the shore erosion can affect other CB segments, it affects the local segments to a greater degree because much of the simulated shore erosion load has deposited in the shallow water region prior to wider transport.

Tables 3-5 also contain the results from tidal fresh, oligohaline, and mesohaline CB segments of the Patuxent River. The results, such as changes of ISS and TSS *vs.* Kd change among the source-sensitivity scenarios, are consistent with those from the mainstem CB segments.

Geographically Isolated Sediment Loading Sources. Figures 7-9 plot estimated ISS concentrations in three of the WQSTM's bottom cells of the tidal Patuxent River from various sediment load sources during the August 7-25, 2004 period. The cells can be located in Figure 3 and are designated by the star symbol and accompanied by their five-digit cell identification numbers. In the legend "Region 1" designates the sediment load from Region 1 only, while "Regions 1 + 2 + 3" represent the sediment from combined sources of Regions 1, 2, and 3. The contribution of sediment from a specific source region can be calculated from concentration differences between two combined sources.

Figure 7 represents ISS concentrations in cell 17741 at the lower end of Region 2 in the middle tidal fresh portion of the Patuxent River. The ISS values are almost the identical, i.e., the regional symbols overlap in the plot for sediment loads from all the regions until about August 12. This indicates that Regions 2, 3, 4, 5, and 6 have little effect on cell 17741 of the tidal fresh during this period. Region 1's source (from the Patuxent watershed above the fall line) has a significant influence on ISS concentrations

TABLE 3. Kd and Percent Kd Changes in Source-Type Scenarios against the Base Scenario. Units in 1 m^{-1} or percent change (% Δ).

CB Segment	Base	No Ocean		No Resuspension		No Shore Erosion		No Major River		No Watershed	
	Kd	Kd	% Δ	Kd	% Δ	Kd	% Δ	Kd	% Δ	Kd	% Δ
CB1TF	1.78	1.73	-2.75	1.41	-20.97	1.64	-7.60	1.18	-33.57	1.13	-36.37
CB2OH	1.99	1.80	-9.50	0.95	-52.21	1.74	-12.49	1.39	-30.32	1.25	-37.21
CB3MH	1.77	1.62	-8.88	0.95	-46.12	1.61	-8.97	1.48	-16.46	1.32	-25.60
CB4MH	1.43	1.30	-9.09	0.88	-38.46	1.24	-12.90	1.33	-6.53	1.19	-16.61
CB5MH	1.08	0.96	-10.81	0.66	-39.21	0.95	-12.23	1.03	-4.70	0.90	-16.39
CB6PH	1.06	0.88	-16.74	0.60	-43.29	0.98	-7.38	1.02	-3.32	0.84	-20.82
CB7PH	1.06	0.86	-19.21	0.65	-38.91	1.00	-6.12	1.03	-2.63	0.82	-22.49
CB8PH	0.97	0.77	-20.57	0.60	-38.05	0.93	-4.14	0.92	-4.97	0.71	-26.22
PAXMH	1.60	1.48	-7.69	0.94	-40.94	1.28	-19.69	1.43	-10.40	1.26	-21.23
PAXOH	3.42	3.17	-7.36	2.03	-40.67	3.31	-3.07	2.37	-30.71	1.93	-43.58
PAXTF	4.83	5.55	14.88	3.84	-20.60	4.83	0.00	3.09	-36.11	2.51	-48.09

Note: CB, Chesapeake Bay.

TABLE 4. TSS and Percent TSS Changes in Source-Type Scenarios against the Base Scenario. Units in mg/l or percent change (% Δ).

CB Segment	Base	No Ocean		No Resuspension		No Shore Erosion		No Major River		No Watershed	
	TSS	TSS	% Δ	TSS	% Δ	TSS	% Δ	TSS	% Δ	TSS	% Δ
CB1TF	13.6	14.6	7.11	9.4	-30.88	12.4	-9.13	6.6	-51.55	6.0	-55.59
CB2OH	14.8	12.7	-14.08	4.2	-71.27	12.3	-16.79	8.2	-44.48	6.8	-53.82
CB3MH	12.4	10.7	-13.54	4.3	-65.22	10.7	-13.76	9.3	-24.89	7.6	-38.17
CB4MH	10.4	8.9	-14.04	4.5	-56.74	8.3	-20.42	9.3	-10.29	7.7	-25.44
CB5MH	8.9	7.4	-16.95	3.6	-59.54	7.2	-19.43	8.2	-7.55	6.6	-25.82
CB6PH	8.6	6.4	-26.26	3.0	-65.50	7.6	-11.78	8.2	-5.48	5.8	-32.70
CB7PH	8.7	6.1	-30.18	3.6	-58.38	7.9	-9.46	8.4	-4.15	5.7	-35.19
CB8PH	12.2	8.3	-32.42	5.0	-58.82	11.4	-6.65	11.3	-8.06	7.2	-41.33
PAXMH	12.7	11.2	-11.70	5.4	-57.89	9.0	-29.19	10.7	-15.96	8.7	-31.61
PAXOH	21.5	19.4	-9.79	10.3	-52.37	20.7	-3.96	12.7	-40.94	9.2	-57.20
PAXTF	38.1	47.5	24.84	28.1	-26.19	38.1	0.00	20.7	-45.66	15.2	-60.18

Note: TSS, total suspended solids; CB, Chesapeake Bay.

TABLE 5. ISS and Percent ISS Changes in Source-Type Scenarios against the Base Scenario. Units in mg/l or percent change (% Δ).

CB Segment	Base	No Ocean		No Resuspension		No Shore Erosion		No Major River		No Watershed	
	ISS	ISS	% Δ	ISS	% Δ	ISS	% Δ	ISS	% Δ	ISS	% Δ
CB1TF	8.7	9.3	7.20	4.7	-45.92	7.6	-12.77	2.16	-75.19	1.32	-84.83
CB2OH	11.6	9.6	-17.14	1.1	-90.82	9.2	-20.27	5.14	-55.64	3.86	-66.70
CB3MH	8.7	7.0	-19.33	0.4	-95.69	7.1	-18.48	5.62	-35.61	3.96	-54.55
CB4MH	6.8	5.3	-21.96	0.7	-89.49	4.8	-28.96	5.75	-15.70	4.13	-39.38
CB5MH	5.8	4.3	-26.42	0.4	-92.27	4.3	-26.23	5.14	-11.44	3.49	-39.87
CB6PH	6.2	3.9	-36.87	0.6	-90.67	5.3	-14.33	5.73	-7.26	3.38	-45.39
CB7PH	6.5	3.8	-40.72	1.5	-77.04	5.8	-10.15	6.14	-5.16	3.44	-46.95
CB8PH	9.9	5.9	-40.19	2.7	-72.52	9.1	-7.51	8.90	-9.77	4.84	-50.92
PAXMH	9.5	8.0	-15.62	2.0	-79.29	5.8	-38.36	7.40	-21.70	5.44	-42.44
PAXOH	15.4	13.4	-13.22	3.0	-80.32	14.5	-5.74	5.55	-63.99	1.57	-89.83
PAXTF	26.2	35.3	34.74	15.2	-41.95	26.2	-0.01	6.55	-75.00	0.04	-99.85

Note: ISS, inorganic suspended solids; CB, Chesapeake Bay.

at 5-17 mg/l. The Region 2 source has a significant effect around August 14 by contributing sediment loads to raise the bottom cell ISS concentration as

high as 75 mg/l. This is related to a storm with strong shore erosion and runoff from the Coastal Plain watershed areas.

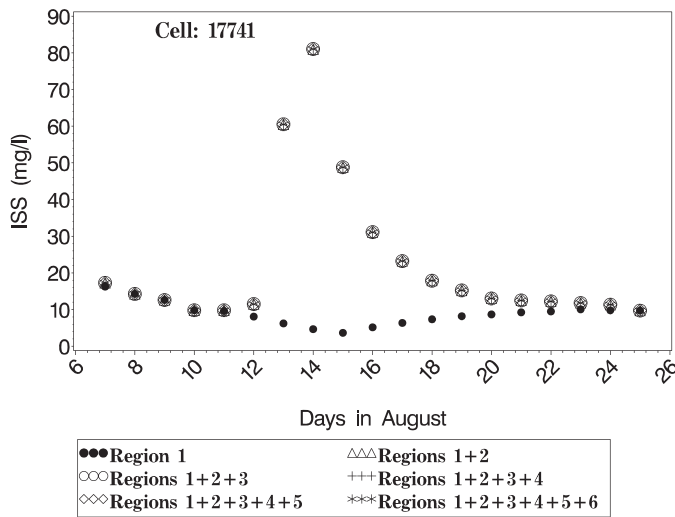


FIGURE 7. Computed Inorganic Suspended Solids Concentration in a Model Cell in the Upper Patuxent River before and after an August Storm. Concentrations are shown for combinations of solids load from multiple regional sources.

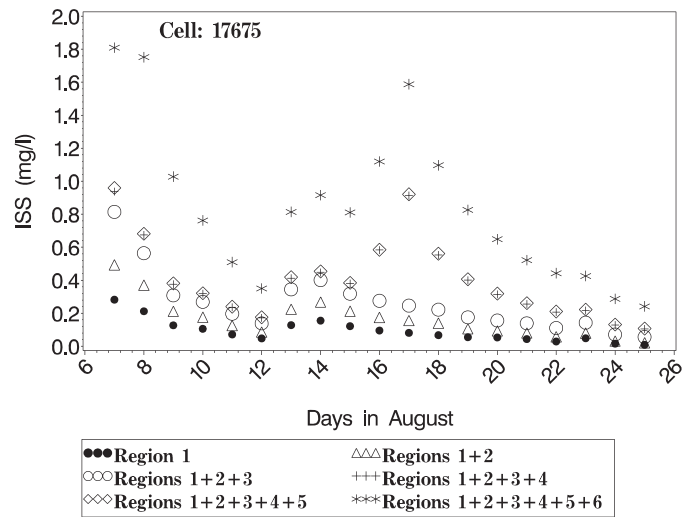


FIGURE 8. Computed Inorganic Suspended Solids Concentration in a Model Cell in the Middle Patuxent River before and after an August Storm. Concentrations are shown for combinations of solids load from multiple regional sources.

Figure 8 shows ISS concentrations in cell 17675 at the lower end of Region 3 in the oligohaline portion of the river. The sediment source from the major rivers (Region 1) has a minor effect, while the sediments from all other regions have discernible influences. The sediment from Region 6, representing the entire tidal Bay beyond the mouth of the Patuxent, has more influence on bottom cells than surface cells because the sediment from Region 6 is mainly transported in bottom water layers.

In cell 17895 (at lower Region 5 of PAXMH, closer to the mouth), the sediment loads from Regions 5 and 6 become the most prominent, and Region 4 has a greater influence than Regions 1, 2, and 3 (Figure 9).

The sediment loads from Regions 1, 2, and 3 are primarily from the major rivers or Coastal Plain watershed areas adjacent to the tidal Bay, while the sediment from Regions 4 and 5 are mainly from shore erosion as well as the Coastal Plain watershed sediment load. Sand, silt, and clay were analyzed in the ISS composition. From the sediment source-sensitivity scenarios and geographic loading scenarios, it was found that clay and silt are the main components (95%) in ISS. Discernible effects from sand are mainly in tidal fresh and in some nearshore areas, especially during high precipitation/flow periods.

The above transport of ISS can also be simulated by a conservative tracer with multiple grain sizes and settling rates (Wang *et al.*, 2001). However, the geographic loading scenarios applied in this article have the advantage of being able to simulate water clarity by the effect of nutrient/chlorophyll besides simulating the inorganic solids as described in Wang *et al.* (2004).

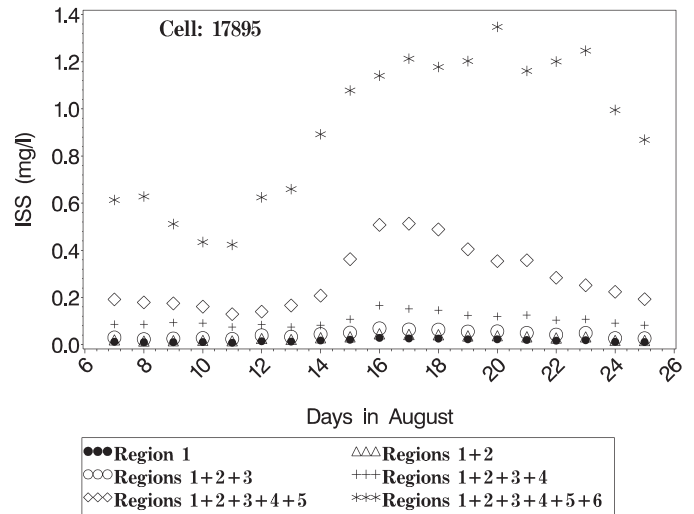


FIGURE 9. Computed Inorganic Suspended Solids Concentration in a Model Cell in the Lower Patuxent River before and after an August Storm. Concentrations are shown for combinations of solids load from multiple regional sources.

Application in Water Clarity TMDL Assessment

Using insights and elements from the above analyses the relative effects of sediment and nutrient loads from diverse sources on K_d in specific CB segments can be assessed. The following steps can be used to estimate sediment and nutrient load reduction to achieve the water clarity goal for the CB water clarity TMDL.

Step 1. Based on the required (minimum) percent light through water (i.e., $f = I/I_0$) and the application

depth Z for a CB segment, use Equation (1) to get the maximum allowable K_d : allowable $K_d_{max} = -\ln(f)/Z$.

Step 2. Access the average K_d , TSS, and chlorophyll- a under the current condition in each CB segment's water. If a CB segment has $K_d >$ allowable K_d_{max} , a water clarity TMDL will be imposed. The required K_d improvement, dK_d , equals the current K_d subtracted by allowable K_d_{max} .

Step 3. Based on the results from the differential sediment and nutrient loading scenarios (Table 2), construct a plot similar to Figure 6 for the CB segment.

Step 4. On Figure 6, use the current loads (either nutrient or sediment, depending on the slope of K_d isopleths) to intersect the current K_d isopleths, getting a point, X. Note: If the calculations are exact, the lines of nutrient and sediment loads will meet at the current K_d isopleths. Model errors will cause them not to meet at the current K_d isopleths.

Step 5. Any line from point X to the allowable K_d_{max} isopleths is a candidate path for nutrient and sediment load reductions. The path with the shortest distance can be most cost effective. From our analysis, for many tidal fresh or oligohaline, a nearly vertical line, i.e., achievement of the clarity standard primarily through sediment reductions alone can be cost effective.

Step 6. Determine percent sediment and/or nutrient load reductions to achieve the K_d target. In order for all CB segments to have K_d equal or less than their K_d_{max} , we need to pay attention to the CB segment that has greatest required dK_d .

Step 7. Finally, the WQSTM is run using the proposed sediment and nutrient loads as input to confirm the target CB segments meet the K_d requirements. A safety factor may also be applied due to model uncertainty.

The above approach is based on bay-wide reductions derived from Table 2 in Step 3 and it could be more cost efficient to allocate more load reduction to the basins that have greater impact on the problematic CB segment. For this purpose, we need to assess relative importance of shore erosion, resuspension, major river input, etc. on key segments, using the aforementioned source-type model scenarios and the geographically isolated loading scenarios. Accordingly, in Step 3 we would use the scenario set with local load reduction for a target CB segment to build Figure 6.

CONCLUSIONS

K_d is closely related to *in situ* TSS and chlorophyll- a concentrations. The relative importance of

TSS *vs.* chlorophyll- a concentrations to K_d varies among the 102 CB segments. In general, in tidal fresh and oligohaline CB segments K_d is more correlated to TSS, i.e., the strength of a linear relationship between K_d and TSS is greater than that of K_d and chlorophyll- a . In mesohaline and polyhaline CB segments K_d is more correlated with chlorophyll- a . The differences are primarily due to the influence of the major river sediment source. Light attenuation (K_d) in some tributaries is more closely correlated with TSS, while in other tributaries it is more closely correlated with chlorophyll- a . This is mainly due to tributary features that have different sediment *vs.* nutrient inputs. In general, the salinity characteristic is stronger than tributary characteristics in K_d correlations to TSS *vs.* chlorophyll- a .

The correlation between K_d with sediment and nutrient loads is more complicated than the correlation of K_d with *in situ* TSS and chlorophyll- a concentrations. This is mainly due to seasonal variation in the diverse watershed loading sources, the processing, fate, and transport of the nutrient loads in the estuary and the lag time of response of TSS and chlorophyll- a concentrations in tidal water to the watershed loads. The tidal fresh and oligohaline areas have shorter lag times, and show slightly more correlation of K_d with watershed loads.

The modeled set of differential sediment and nutrient load scenarios provide information on the relative contributions of sediment and nutrient loads on light attenuation in the CB segments. The chart (i.e., Figure 6) developed in this study can be used to estimate sediment and nutrient load reductions that will achieve a target K_d . The analysis of K_d sensitivity to different sediment sources provides information on the relative importance of sediment source types (such as resuspension, ocean input, shore erosion, major river sediment loads, and other watershed sediment loads) for each of the CB segments. Sediment loads from the watershed affect most CB segments, and the major river sediment loads are an important source particularly at the point of discharge of the major river systems, which influence adjacent tidal fresh and oligohaline CB segments. Ocean sediment loads influence primarily the lower Bay CB segments near the mouth of the Chesapeake. Shore eroded sediment loads and resuspension have their greatest influence in an area local to the loads.

The set of geographic isolated sediment loading scenarios provides information on the relative effect of sediment from distributed areas on K_d and sediment concentrations in specific water bodies. The Patuxent River example shows the tidal fresh CB segment receives sediment mainly from the major river discharge, with the downstream Patuxent region receiving sediment from both the upstream

and from areas outside the Patuxent. The local sediment source is usually the most influential sediment load on K_d indicating the usually limited transport of the suspended sediment.

Combining monitoring and modeled analyses provides useful information to design cost-effective nutrient and sediment load reductions for the improvement of water clarity.

ACKNOWLEDGMENTS

We appreciate the valuable comments and professional input from the reviewers and support from the Chesapeake Bay Modeling Workgroup, and we also thank Howard Weinberg of the University of Maryland for GIS assistance with the figures.

LITERATURE CITED

- Baldizar, J.M. and N.B. Rybicki, 2006. Primary Factors Affecting Water Clarity at Shallow Water Sites Throughout the Chesapeake and Maryland Coastal Bays. *In*: F. Simoes (Editor), Proceedings of the 8th Federal Interagency Sedimentation Conference, April 2-4, Reno, Nevada, pp. 1027-1034.
- Batiuk, R.A., P. Bergstrom, M. Kemp, E. Koch, L. Murray, J.C. Stevenson, R. Bartleson, V. Carter, N.B. Rybicki, J.M. Landwehr, C. Gallegos, L. Karrh, M. Naylor, D. Wilcox, K.A. Moore, S. Ailstock, and M. Teichberg, 2000. Chesapeake Bay Submerged Aquatic Vegetation Water Quality and Habitat-Based Requirements and Restoration Targets: A Second Technical Synthesis. CBP/TRS 245/00 EPA 903-R-00-014. USEPA Chesapeake Bay Program, Annapolis, Maryland.
- Bicknell, B.R., J.C. Imhoff, J.L. Kittle, A.D. Donigian, and R.C. Johanson, 1997. Hydrological Simulation Program – FORTRAN, User's Manual for Version 11. Prepared for NERL, US Environmental Protection Agency, Athens, Georgia. EPA/600/R-97/080, 755 pp.
- CEC (Chesapeake Executive Council), 2000. Chesapeake Bay Agreement, 2000 Amendments. Chesapeake Executive Council, Annapolis, Maryland.
- Cerco, C.F., S.C. Kim, and M. Noel, 2010. The 2010 Chesapeake Bay Eutrophication Model. A report to USEPA Chesapeake Bay Program, US Army ERDC, Vicksburg, Mississippi.
- Cerco, C.F. and M. Noel, 2004. The 2002 Chesapeake Bay Eutrophication Model. US Army Corps of Engineers, prepared for USEPA Chesapeake Bay Program, Annapolis, Maryland. EPA-903-R-04-004.
- Cerco, C.F. and M.R. Noel, this issue. Twenty-One-Year Simulation of Chesapeake Bay Water Quality Using the CE-QUAL-ICM Eutrophication Model. *Journal of the American Water Resources Association*, doi: 10.1111/jawr.12107. EPA-903-R-13-011, CBP/TRS-317-13-10.
- Cerco, C.F., M.R. Noel, and P. Wang, this issue. The Shallow-Water Component of the Chesapeake Bay Environmental Model Package. *Journal of the American Water Resources Association*, doi: 10.1111/jawr.12106. EPA-903-R-13-009, CBP/TRS-315-13-8.
- Dennison, W.C., R.J. Orth, K.A. Moore, J.C. Stevenson, V. Carter, S. Kollar, P. Bergstrom, and R.A. Batiuk, 1993. Assessing Water Quality with Submerged Aquatic Vegetation. *BioScience* 43:86-94.
- Gallegos, L.C., 2001. Calculating Optical Water Quality Targets to Restore and Protect Submerged Aquatic Vegetation: Overcoming Problems in Partitioning the Disuse Attenuation Coefficient for Photosynthetically Active Radiation. *Estuaries* 24(3):381-397.
- Gallegos, L.C. and P.W. Bergstrom, 2005. Effects of a *Prorocentrum* Minimum Bloom on Light Availability for and Potential Impact on Submersed Aquatic Vegetation in Upper Chesapeake Bay. *Harmful Algae* 4:553-574.
- Gallegos, L.C., T.E. Jordan, A.H. Hines, and D.E. Weller, 2005. Temporal Variability of Optical Properties in a Shallow, Eutrophic Estuary: Seasonal and Interannual Variability. *Estuarine Coastal and Shelf Science* 64:156-170.
- Gallegos, C.L., P.J. Werdell, and C.R. McClain, 2011. Long-Term Changes in Light Scattering in Chesapeake Bay Inferred from Secchi Depth, Light Attenuation, and Remote Sensing Measurements. *Journal of Geophysical Research*. 117:1-19.
- Jerlov, N.G., 1976. *Marine Optics* (Second Edition). Elsevier Scientific Publishing Co, Amsterdam, The Netherlands.
- Kemp, W.M., R. Batiuk, R. Bartleson, P. Bergstrom, V. Carter, G. Gallegos, W. Hunley, L. Karrh, E. Koch, J. Landwehr, K. Moore, L. Murray, M. Naylor, N. Rybicki, J.C. Stevenson, and D. Wilcox, 2004. Habitat Requirements for Submerged Aquatic Vegetation in Chesapeake Bay: Water Quality, Light Regime, and Physical-Chemical Factors. *Estuaries* 27(3):363-377.
- Kemp, W.M., W.R. Boynton, R.R. Twilley, J.C. Stevenson, and L.G. Ward, 1984. Influences of Submersed Vascular Plants on Ecological Processes in Upper Chesapeake Bay. *In*: Estuaries as Filters, V.S. Kennedy (Editor). Academic, New York City, New York, pp. 367-394.
- Kirk, J.T.O., 1983. *Light and Photosynthesis in Aquatic Ecosystems*. Cambridge University Press, Cambridge, United Kingdom, 401 pp.
- Koroncai, R., L.C. Linker, J. Sweeny, and R. Batiuk, 2003. Setting and Allocating the Chesapeake Bay Basin Nutrient and Sediment Loads. USEPA Chesapeake Bay Program Office, Annapolis, Maryland.
- Linker, L.C., R.A. Batiuk, G.W. Shenk, and C.F. Cerco, this issue. Development of the Chesapeake Bay Watershed Total Maximum Daily Load Allocation. *Journal of the American Water Resources Association*, doi: 10.1111/jawr.12105. EPA-903-R-13-003, CBP/TRS-309-13-2.
- Lubbers, L., W.R. Boynton, and W.M. Kemp, 1990. Variations in Structure of Estuarine Fish Communities in Relation to Abundance of Submersed Vascular Plants. *Marine Ecology Progress Series* 65:1-14.
- Nash, J.E. and J.V. Sutcliffe, 1970. River Flow Forecasting Through Conceptual Models: A Discussion of Principles. *Journal of Hydrology* 10:282-290.
- Officer, C.B., R.B. Biggs, J.L. Taft, L.E. Cronin, M.A. Tyler, and W.R. Boynton, 1984. Chesapeake Bay Anoxia: Origin, Development and Significance. *Science* 233:22-27.
- Orth, R.J. and J. van Montfrans, 1990. Utilization of Marsh and Seagrass Habitats by Early Stages of *Callinectes sapidus*: A Latitudinal Perspective. *Bulletin of Marine Science* 46:126-144.
- Redfield, A., B. Ketchum, and F. Richards, 1966. The Influence of Organism on the Composition of Sea-Water. *In*: The Sea, Volume II, M.N. Hill (Editor). Interscience Publishers, New York City, New York, pp. 26-48.
- Shenk, G.W. and L.C. Linker, this issue. Development and Application of the 2010 Chesapeake Bay Watershed Total Maximum Daily Load Model. *Journal of the American Water Resources Association*, doi: 10.1111/jawr.12109. EPA-903-R-13-004, CBP/TRS-310-13-3.
- Smith, R.C., K.S. Baker, and J.B. Fahy, 1983. Effects of Suspended Sediments on Penetration of Solar Radiation into Natural Waters. U.S. Environmental Protection Agency Report EPA-600/3-83-060, USEPA, Athens, Georgia, 42 pp.
- Stefan, H.G., J.J. Cardoni, F.R. Schiebe, and C.M. Cooper, 1983. Model of Light Penetration in a Turbid Lake. *Water Resources Research*. 19:109-120.
- Tango, P.J. and R.A., Batiuk, this issue. Deriving Chesapeake Bay Water Quality Standards. *Journal of the American Water*

- Resources Association, doi: 10.1111/jawr.12108. EPA-903-R-13-005, CBP/TRS-311-13-4.
- USEPA (U.S. Environmental Protection Agency), 2003. Ambient Water Quality Criteria for Dissolved Oxygen, Water Clarity and Chlorophyll *a* for the Chesapeake Bay and Its Tidal Tributaries. EPA 903-R-03-002. U.S. Environmental Protection Agency, Region 3, Chesapeake Bay Program Office, Annapolis, Maryland.
- USEPA (U.S. Environmental Protection Agency), 2004. Technical Support Document for Identification of Chesapeake Bay Designated Uses and Attainability, 2004 Addendum. EPA 903-R-04-008. U.S. Environmental Protection Agency, Region 3, Chesapeake Bay Program Office, Annapolis, Maryland.
- USEPA (U.S. Environmental Protection Agency), 2007. Ambient Water Quality Criteria for Dissolved Oxygen, Water Clarity and Chlorophyll *a* for the Chesapeake Bay and Its Tidal Tributaries, 2007 Addendum. EPA 903-R-07-003. U.S. Environmental Protection Agency, Region 3, Chesapeake Bay Program Office, Annapolis, Maryland.
- USEPA (U.S. Environmental Protection Agency), 2010. Chesapeake Bay Total Maximum Daily Load for Nitrogen, Phosphorus and Sediment. U.S. Environmental Protection Agency Chesapeake Bay Program Office, Annapolis, Maryland. <http://www.epa.gov/reg3wapd/tmdl/ChesapeakeBay/tmdlexec.html>, accessed March 2012.
- Wang, P., L.C. Linker, and R. Batiuk, 2002. Surface Analysis of Water Quality Response to Load. *In*: M.L. Spaulding (Editor), Estuarine and Coastal Modeling: Proceedings 7th International Conference, November 2001, St. Pete Beach, Florida, ISBN: 0-7844-0628-6, pp. 566-584.
- Wang, P., L.C. Linker, R. Batiuk, and G. Shenk, 2001. Assessment of Impact of Storm on Point Source Pollutant Transport in Estuary by Dissolved Tracer Modeling. *Water Quality and Ecosystem Modeling* 1:253-269.
- Wang, P., L.C. Linker, and G. Shenk, 2004. Assessment of Relative Effect of Nutrient Loads from Different Sub-Watershed to a Specific Water-Body. *In*: S. Fujii, K. Yamada, and T. Kunimatsu (Editors), Proceedings of 8th International Conference on Diffuse/Nonpoint Pollution, October 2004, Kyoto, Japan, PII, pp. 9-16.